A Multi-Objective Evolutionary Hyper-heuristic based on Multiple Indicator-based Density Estimators

Jesús Guillermo Falcón-Cardona
Computer Science Department
CINVESTAV-IPN
Mexico, Mexico City 07360
jfalcon@computacion.cs.cinvestav.mx

Carlos A. Coello Coello
Computer Science Department
CINVESTAV-IPN
Mexico, Mexico City 07360
ccoello@cs.cinvestav.mx

ABSTRACT

In recent years, Indicator-based Multi-Objective Evolutionary Algorithms (IB-MOEAs) have become a relatively popular alternative for solving multi-objective optimization problems. IB-MOEAs are normally based on the use of a single performance indicator. However, the effect of the combination of multiple performance indicators for selecting solutions is a topic that has rarely been explored. In this paper, we propose a hyper-heuristic which combines the strengths and compensates for the weaknesses of four density estimators based on $R2$, IGD^+, ϵ^+ and Δ_p. The selection of the indicator to be used at a particular moment during the search is done using online learning and a Markov chain. Additionally, we propose a novel framework that aims to reduce the computational cost involved in the calculation of the indicator contributions. Our experimental results indicate that our proposed approach can outperform state-of-the-art MOEAs based on decomposition (MOEA/D) reference points (NSGA-III) and the $R2$ indicator ($R2$-EMOA) for problems with both few and many objectives.

CCS CONCEPTS

• **Theory of computation → Bio-inspired optimization**; • **Computing methodologies → Continuous space search**;

KEYWORDS

Multi-objective Optimization, Quality Indicators, Hyper-heuristics

ACM Reference Format:
Jesús Guillermo Falcón-Cardona and Carlos A. Coello Coello. 2018. A Multi-Objective Evolutionary Hyper-heuristic based on Multiple Indicator-based Density Estimators. In *GECCO '18: Genetic and Evolutionary Computation Conference, July 15–19, 2018, Kyoto, Japan.* ACM, New York, NY, USA, 8 pages. https://doi.org/10.1145/3205455.3205463

1 INTRODUCTION

In this work, we focus on multi-objective optimization problems (MOPs) which involve the simultaneous optimization of several, often conflicting, objective functions of the form:

$$\min_{\vec{x}\in\Omega} \vec{F}(\vec{x}) = (f_1(\vec{x}), f_2(\vec{x}), \ldots, f_m(\vec{x}))^\intercal, \tag{1}$$

where $\vec{x}$ is the vector of decision variables, $\Omega \subseteq \mathbb{R}^n$ is the decision variable space and $\vec{F}(\vec{x})$ is the vector of m (≥ 2) objective functions ($f_i : \mathbb{R}^n \mapsto \mathbb{R}$) that belongs to the feasible objective space $\Psi \subseteq \mathbb{R}^m$. MOPs having four or more objective functions are called many-objective optimization problems (MaOPs) [14]. Solving a MOP involves finding the best possible trade-offs among its objectives (i.e., finding solutions in which an objective cannot be improved without worsening another). The particular set that yields the optimum values is known as the Pareto Optimal Set ($\mathcal{P}^*$) and its image in objective space is known as the Pareto Optimal Front ($\mathcal{PF}^*$).

Multi-Objective Evolutionary Algorithms (MOEAs) are population-based and gradient-free metaheuristics that have been successfully applied to solve MOPs [7]. MOEAs are inspired by the natural evolution of organisms i.e., they drive the population to $\mathcal{PF}^*$ by selecting the fittest individuals at each generation. According to Zitzler et al. [29], the main goals of MOEAs, regarding their Pareto front approximations, are the following: (1) to achieve convergence of the solutions, (2) to generate a uniform distribution of solutions, and (3) to maximize the extent of the generated solutions. Commonly, convergence is achieved by an environmental selection based on Pareto dominance[1], while diversity and spread are handled by a density estimator (DE).

Quality indicators[2] (QIs) are functions that quantitatively determine how good is an approximation set generated by an MOEA [32]. QIs aim to assess the desired features of approximation sets, i.e., convergence, distribution, spread and a combination of them [16, 22]. Regarding convergence QIs, an important property is Pareto-compliance. A (weakly) Pareto-compliant QI guarantees that one algorithm's indicator values are better (or at least not worse) than another in case the approximation sets of the former (weakly) dominates the other's. Table 1 introduces the features of some remarkable state-of-the-art convergence QIs.

Regarding MaOPs, the selection pressure of Pareto-based MOEAs dilutes due to the exponential increase of solutions preferred by Pareto dominance. In furtherance of tackling this issue, indicator-based MOEAs (IB-MOEAs) have become a popular alternative

GECCO '18, July 15–19, 2018, Kyoto, Japan

ACM ISBN 978-1-4503-5618-3/18/07…$15.00
https://doi.org/10.1145/3205455.3205463

[1] Given $\vec{x}, \vec{y} \in \Omega$, we say that $\vec{x}$ *dominates* $\vec{y}$ (denoted as $\vec{x} \prec \vec{y}$) if and only if $f_i(\vec{x}) \leq f_i(\vec{y})$ for $i = 1, \ldots, m$ and $\exists j \in \{1, \ldots, m\} : f_j(\vec{x}) < f_j(\vec{y})$. In case, $f_i(\vec{x}) \leq f_i(\vec{y})$ for all $i \in \{1, \ldots, m\}$, $\vec{x}$ is said to *weakly dominate* $\vec{y}$ (denoted as $\vec{x} \preceq \vec{y}$).

[2] Let $\mathcal{A} \subset \mathcal{PF}^*$ be an approximation set. A k-ary quality indicator is a function $I : (\mathcal{A}_1, \ldots, \mathcal{A}_k) \mapsto \mathbb{R}$ which assigns a real value to a vector of k approximation sets.

Table 1: Features of some state-of-the-art convergence QIs.

Indicator	Acronym	Pareto-compliant	Required information	Ref.
Hypervolume	HV	Strictly	Reference point	[31]
R2	*R2*	Weakly	Set of weight vectors and utility function	[3]
Modified Inverted Generational Distance	IGD^+	Weakly	Reference set	[13]
Additive ϵ indicator	ϵ^+	Weakly	Reference set	[32]
Averaged Hausdorff Distance	Δ_p	No	Reference set $p > 0$	[25]

[2, 4, 30]. IB-MOEAs usually exploit the properties of a single indicator as the backbone of three different mechanisms: (1) environmental selectors (IB-ES), (2) density estimators (IB-DE), and (3) archivers (IB-AR). The hypervolume indicator (HV) has been extensively employed by IB-MOEAs [1, 2] because it is the only unary indicator that is known to be strictly Pareto compliant. However, since its computational cost significantly increases with the number of objectives, its use eventually becomes prohibitive in MaOPs. In contrast, other less-expensive indicators have been successfully employed by IB-MOEAS (e.g., *R2* [3], IGD^+ [13], Δ_p [25] and ϵ^+ [32]) at the expense of using an indicator with weaker mathematical properties.

It is worth noting that every single indicator, when coupled to an MOEA, imposes a specific bias in objective space regarding convergence, distribution and spread [15, 20]. On the one hand, HV ensures finding uniformly distributed solutions in linear Pareto fronts, but it presents a bias to points close to the Pareto front's knee.[3] On the other hand, *R2* promotes uniformly distributed solutions in concave Pareto fronts while this is not possible in disconnected fronts because the indicator is defined from a set of convex weight vectors. Similar issues arise for the other indicators mentioned before. Hence, by the No-Free Lunch Theorem (NFL), an IB-MOEA cannot show a good performance in all types of MOPs. An alternative approach to mitigate this problem is the use of hyper-heuristics which are search methods or learning mechanisms for selecting or generating heuristics to solve computational search problems [5].

In this paper, we propose what we believe to be the first multi-indicator MOEA which is focused on exploiting the strengths and compensating for the weaknesses of density estimators based on the indicators: *R2*, IGD^+, Δ_p and ϵ^+. In other words, we investigate the effect of the combination of the previously mentioned indicators. A hyper-heuristic using online learning and a Markov chain decides which of these IB-DEs is to be used at a particular moment through the search process. Additionally, we propose a novel framework that reduces the computational cost of calculating the indicator contributions. All these mechanisms are integrated into a steady-state MOEA that uses Pareto dominance for its environmental selection.

The remainder of this paper is organized as follows. Section 2 briefly introduces the most relevant related work on Multi-Indicator MOEAs. Section 3 provides the mathematical definition of the selected indicators. Our proposed approach is described in Section 4. Section 5 depicts our experimental results and, finally, the conclusions and future work are highlighted in Section 6.

[3]The knee of the Pareto front is the region which is closer to the ideal point defined as $\vec{z}^* \in \mathbb{R}^m$, where $z_i^* = \min_{\vec{x} \in \Omega} f_i(\vec{x})$.

2 RELATED WORK

The first IB-MOEA was proposed by Knowles and Corne [17], and since then, several single-indicator based MOEAs have been introduced. However, to the authors' best knowledge, only four isolated Multi-Indicator-based MOEAs (MIB-MOEAs) have been proposed so far. In this section, we briefly review two remarkable IB-MOEAs, and we describe the currently available MIB-MOEAs.

The S-Metric Selection Evolutionary Multi-Objective Algorithm (SMS-EMOA) [2] is a steady-state MOEA that employs an IB-DE based on the HV indicator. First, the population is divided into nondominated layers through the nondominated sorting algorithm [8]. In case the last layer has more than one individual, the one having the worst HV contribution is deleted. SMS-EMOA maximizes the HV indicator through the evolutionary process which is directly related to finding Pareto optimal solutions because HV is strictly Pareto-compliant. However, its use is restricted to low-dimensional MOPs. As an alternative to the high computational cost of SMS-EMOA, Brockhoff et al. [4] proposed the *R2*-EMOA. Instead of employing the HV contribution to delete an individual, *R2*-EMOA uses the *R2* contribution. The complexity of computing the *R2* contributions of N individuals is substantially less than calculating the HV contributions. Hence, *R2*-EMOA can solve MaOPs in a considerably lower time than SMS-EMOA.

The first MIB-MOEA was the Boosting Indicator-Based Evolutionary Algorithm (BIBEA) [23] that was proposed by Phan and Suzuki in 2011. BIBEA incorporates a parent selection mechanism that aggregates the indicators HV and ϵ^+ using the AdaBoost algorithm. Through an offline learning process that uses Pareto optimal points of a given MOP, AdaBoost searches for a set of weights that assigns preferences to each of the indicator-based parent tournament selection operators such that the error related to the selection of Pareto or non-Pareto optimal solutions is minimized. Having computed the weights, BIBEA employs them to construct its multi-indicator parent selection mechanism. Unfortunately, the authors only provided an analysis of convergence and diversity of BIBEA, leaving the comparison with other MOEAs out of the study. One year later, Phan et al. [24] introduced a variant of BIBEA, called BIBEA-P. The three main differences concerning BIBEA are the following: (1) AdaBoost is replaced by Pdi-Boosting, (2) a boosting indicator-based environmental selection is added, and (3) a comparison with other MOEAs is presented. The new environmental selection uses the indicator that produces the minimum selection error in the training stage. Thus, it is very similar to BIBEA. The experimental results provided by its authors indicated that BIBEA-P could outperform NSGA-II [8], SMS-EMOA [2], and IBEA [30].

Unlike BIBEA and BIBEA-P which are ensemble methods, the Stochastic Ranking-based Multi-Indicator Algorithm (SRA) [18] is an MOEA that aims to balance the search biases of the indicators ϵ^+ and SDE [19]. SRA is a steady-state MOEA that uses the stochastic ranking algorithm as its environmental selection mechanism to sort the population using the two considered indicators as its sorting criteria. After the sorting is done, the worst solution is deleted. The authors show exhaustive experimentation using benchmark

problems in low- and high-dimensional objective spaces, comparing their results with those produced by a wide variety of state-of-the-art MOEAs.

More recently, Hernández and Coello [11] proposed MOMBI-III which is a hyper-heuristic that selects the best utility function for its environmental selection based on the *R2* indicator. Additionally, MOMBI-III uses an IB-DE that calculates the contributions to the s-energy indicator [10] to reduce the joint population of parents and offspring to a specific size. Thus, MOMBI-III combines the effect of *R2* selection and the s-energy density estimation.

3 QUALITY INDICATORS

In this section, we formally define the *R2*, IGD^+, Δ_p and ϵ^+ indicators. In all cases, let $\mathcal{A}$ be an approximation set and $\mathcal{Z}$ be a reference set. m is the dimension of the objective space.

Definition 1 (Unary *R2* indicator). *The unary R2 indicator is defined as follows:*

$$R2(\mathcal{A}, W) = -\frac{1}{|W|} \sum_{\vec{w} \in W} \max_{\vec{a} \in \mathcal{A}} \{u_{\vec{w}}(\vec{a})\} \tag{2}$$

where W is a set of weight vectors and $u_{\vec{w}} : \mathbb{R}^m \mapsto \mathbb{R}$ is a scalarizing function defined by $\vec{w} \in W$ that assigns a real value to each m-dimensional vector.

Definition 2 (IGD^+ indicator). *The IGD^+, for minimization, is defined as follows:*

$$IGD^+(\mathcal{A}, Z) = \frac{1}{|Z|} \sum_{\vec{z} \in Z} \min_{\vec{a} \in \mathcal{A}} d^+(\vec{a}, \vec{z}) \tag{3}$$

where $d^+(\vec{a}, \vec{z}) = \sqrt{\sum_{k=1}^{m} (\max\{a_k - z_k, 0\})^2}$.

Definition 3 (Δ_p indicator). *For a given $p > 0$, the Δ_p is defined as follows:*

$$\Delta_p(\mathcal{A}, Z) = \max\left\{GD_p(\mathcal{A}, Z), IGD_p(\mathcal{A}, Z)\right\}. \tag{4}$$

Δ_p is defined on the basis of two indicators: GD_p and IGD_p which are slight modifications of the indicators Generational Distance (GD) [26] and Inverted Generational Distance (IGD) [6], respectively. These are defined in the following.

Definition 4 (GD_p indicator).

$$GD_p(\mathcal{A}, \mathcal{Z}) = \left(\frac{1}{|\mathcal{A}|} \sum_{\vec{a} \in \mathcal{A}} d(\vec{a}, \mathcal{Z})^p\right)^{1/p}. \tag{5}$$

where $d(\vec{a}, \mathcal{Z}) = \min_{\vec{z} \in \mathcal{Z}} \sqrt{\sum_{i=1}^{m} (a_i - z_i)^2}$.

Definition 5 (IGD_p indicator).

$$IGD_p(\mathcal{A}, \mathcal{Z}) = GD_p(\mathcal{Z}, \mathcal{A}) = \left(\frac{1}{|\mathcal{Z}|} \sum_{\vec{z} \in \mathcal{Z}} d(\vec{z}.\mathcal{A})^p\right)^{1/p}, \tag{6}$$

Definition 6 (Unary ϵ^+ indicator). *The unary ϵ^+-indicator gives the minimum distance by which a Pareto front approximation needs to or can be translated in each dimension in objective space such that a reference set is weakly dominated. Mathematically, it is defined as follows:*

$$\epsilon^+(\mathcal{A}, \mathcal{Z}) = \max_{\vec{z} \in \mathcal{Z}} \min_{\vec{a} \in \mathcal{A}} \max_{1 \le i \le m} \{z_i - a_i\} \tag{7}$$

Figure 1: Memoization structure that stores the minimum and second best value per row of the IGD^+ cost matrix. We assume that $M = N$.

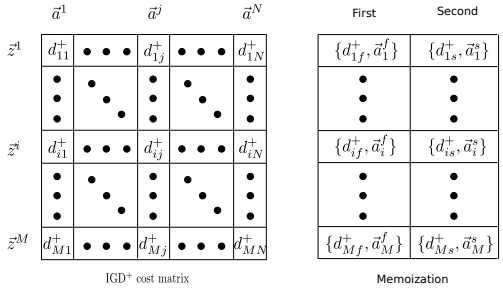

4 OUR PROPOSED APPROACH

In this section, our proposed approach, which is called Multi-Indicator Hyper-heuristic (MIHPS) is described in detail. First, we outline the framework for the fast computation of the contribution to the indicators *R2*, ϵ^+, Δ_p and IGD^+. Then, we describe the hyper-heuristic built from the four IB-DEs and a Markov chain. Finally, the main loop of MIHPS is described.

4.1 Fast Individual Indicator Contribution

The contribution C of a single solution $\vec{a} \in \mathcal{A}$ to an indicator $I \in \{R2, \epsilon^+, \Delta_p, \text{IGD}^+\}$ is defined as follows: $C(\vec{a}, \mathcal{A}) = |I(\mathcal{A}) - I(\mathcal{A} \setminus \{\vec{a}\})|$. For the indicators *R2*, IGD^+, ϵ^+ and Δ_p, it can be easily verified that their computation takes $\Theta(mN^2)$, assuming that $|\mathcal{A}| = |\mathcal{Z}| = |W| = N$. Thus, for a single solution, it takes $\Theta(mN^2) + \Theta(m(N-1)^2) = \Theta(mN^2)$ and for all N solutions it takes $\Theta(mN^3)$. For instance, *R2*-EMOA implements this computational-expensive method for calculating the contributions. Hence, we propose a framework for contribution computation of indicators whose definition involves subproblems of maximization or minimization in pursuance of reducing the previously indicated complexity $\Theta(mN^3)$.

Due to space limitations, we focus the analysis on IGD^+. However, this analysis can be easily adapted for the other indicators previously mentioned. In the left-hand side of Figure 1, we show a cost matrix where $d^+_{ij} = d^+(\vec{a}_j, \vec{z}_i)$ (see Eq. (3)). To compute IGD^+ using this matrix, we look at the minimum value of each row, sum the values and divide the result by N. In case a solution $\vec{a}$, associated with one or more of the minimum values, is removed from $\mathcal{A}$, it will be enough to find the second lowest value in the involved rows. Based on this, a memoization structure is shown at the right-hand side of Figure 1, where each row stores the minimum value, the second minimum and the corresponding pointers to the associated elements in $\mathcal{A}$. Hence, the memoization structure can be used in furtherance of reducing the cost of computing the contributions.

Algorithm 1 describes how to compute the contributions to IGD^+. First, the $\text{IGD}^+(\mathcal{A}, \mathcal{Z})$ value is calculated and assigned to the variable I_{IGD^+}, using the memoization structure. C_i is the variable which will store the individual contribution of the i^{th} element of $\mathcal{A}$. The main loop is outlined in lines 4-12, where the contribution of each solution is computed taking advantage of the memoization structure. ψ is a temporary variable which accumulates the IGD^+ value

of $\mathcal{A} \setminus \{\vec{a}^i\}$. For each element, we only have to determine if it participates in the IGD$^+$ value; if so, we look for the second best value memoized. The obtained values are added to ψ. Finally, ψ is divided by N and assigned as the contribution of the considered element. The complexity of calculating the IGD$^+$ value remains as $\Theta(mN^2)$, and the main loop takes $\Theta(N^2)$. Hence, the required time for computing the individual contributions of all solutions in $\mathcal{A}$ is $\Theta(mN^2)$.

Algorithm 1 Fast IGD$^+$ Individual Contributions

Require: Approximation set $\mathcal{A}$; Reference set $\mathcal{Z}$
Ensure: IGD$^+$ individual contributions
1: Initialize $Memoization$
2: $I_{\text{IGD}^+} \leftarrow \text{IGD}^+(\mathcal{A}, \mathcal{Z}, Memoization)$
3: $\forall i \in \{1, \ldots, |\mathcal{A}|\}, C_i \leftarrow 0$
4: **for** $i = 1$ to N **do**
5: $\quad \psi \leftarrow 0$
6: $\quad$ **for** $j = 1$ to N **do**
7: $\quad\quad$ **if** $Memoization[j].\vec{a}_1^f = \vec{a}^i$ **then**
8: $\quad\quad\quad \psi \leftarrow \psi + Memoization[j].d_{js}^+$
9: $\quad\quad$ **else**
10: $\quad\quad\quad \psi \leftarrow \psi + Memoization[j].d_{jf}^+$
11: $\quad C_i \leftarrow |I_{\text{IGD}^+} - \psi|$
12: **return** $\{C_i\}_{i=1,\ldots,|\mathcal{A}|}$

4.2 Hyper-heuristic

On the basis of the selected indicators, four IB-DEs are defined, namely {IGD$^+$-DE, $R2$-DE, ϵ^+-DE, Δ_p-DE}. This set of IB-DEs is the heuristic pool (H_{pool}) from which the hyper-heuristic chooses the most suitable one depending on the MOP being solved. Our proposed hyper-heuristic is a modified version of the work of McClymont and Keedwell [21] where a Markov chain (MC) is employed. The reasons to use an MC are: (1) its low computational cost, (2) the good performance shown in [21], and (3) the related randomness avoids stagnation on a single IB-DE. The hyper-heuristic requires two steps: (1) performance information collection, and (2) heuristic selection. First, once an IB-DE is selected, it is executed at T_w generations. At each generation, the quality of the produced population is measured using the $R2$ indicator, and each sample is stored in a list associated to the IB-DE in H_{pool}. We decided to use the $R2$ indicator because it is highly correlated to the HV [20]. Algorithm 2 outlines the second step which involves the use of the Markov chain (see Figure 2), the gathered $R2$ values and a control structure denoted as C_{hh}. In the beginning, in line 1, we check if the current IB-DE has been executed. If so, the counter variable of C_{hh} is augmented by one; otherwise, the transition probability is updated, and a new IB-DE is selected (lines 4 to 19). Let i be the last IB-DE executed and j be the current one. Only the probability p_{ij} is updated. Based on the $R2$ values of the current heuristic, we calculate in line 6 a linear regression model where only the slope b and the standard deviation σ of the data are relevant. Using these two values, in lines 7 to 14, we modified p_{ij} in three cases: (1) adding 2α if the slope is non-negative and $\sigma \geq \bar{\sigma}$, where $\bar{\sigma}$ is a threshold value set to 0.1, (2) adding α if the slope is non-negative but $\sigma < \bar{\sigma}$, and (3) subtracting β if the slope is negative. We set $\alpha = \beta = 0.1$. In line 15, we normalized all values in the i^{th} row of the matrix and, finally, we select a new IB-DE using roulette wheel selection.

Algorithm 2 Switch of Heuristics

Require: H_{pool}, C_{hh}, T_w
Ensure: Update current heuristic being executed
1: **if** $C_{hh}.counter < T_w$ **then**
2: $\quad C_{hh}.counter \leftarrow C_{hh}.counter + 1$
3: **else**
4: $\quad i \leftarrow C_{hh}.lastH, j \leftarrow C_{hh}.currentH$
5: $\quad d \leftarrow H_{pool}[j].data$
6: $\quad \{b, \sigma\} \leftarrow ComputeData(d)$
7: $\quad$ **if** $b \geq 0$ and $\sigma \geq \bar{\sigma}$ **then**
8: $\quad\quad C_{hh}.p_{ij} \leftarrow C_{hh}.p_{ij} + 2\alpha$
9: $\quad$ **else if** $b \geq 0$ and $\sigma < \bar{\sigma}$ **then**
10: $\quad\quad C_{hh}.p_{ij} \leftarrow C_{hh}.p_{ij} + \alpha$
11: $\quad$ **else if** $b < 0$ **then**
12: $\quad\quad C_{hh}.p_{ij} \leftarrow C_{hh}.p_{ij} - \beta$
13: $\quad\quad$ **if** $C_{hh}.p_{ij} < 0$ **then**
14: $\quad\quad\quad C_{hh}.p_{ij} \leftarrow 0$
15: $\quad$ Normalize $C_{hh}.p_{it}$, $t = 1, \ldots, |H_{pool}|$
16: $\quad$ Clear data of the current heuristic
17: $\quad C_{hh}.lastH \leftarrow C_{hh}.currentH$
18: $\quad C_{hh}.currentH \leftarrow RouletteWheel()$
19: $\quad C_{hh}.counter \leftarrow 0$

Figure 2: Markov chain and its corresponding transition matrix. Each element $p_{ij} \in [0, 1]$ of the matrix indicates the probability of going from the i^{th} IB-DE to the j^{th} one. For a row i, $\sum_{j=1}^{4} p_{ij} = 1$. All initial transition probabilities p_{ij} are set to $1/|H_{pool}|$.

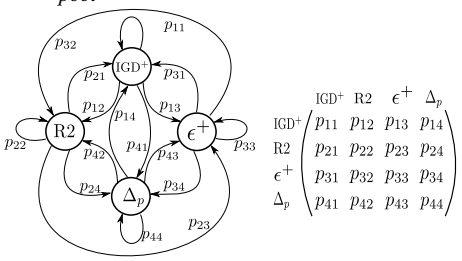

(a) Markov chain (b) Transition matrix

4.3 MIHPS

The general framework of MIHPS is described by Algorithm 3. MIHPS is similar to SMS-EMOA, but the HV-based DE is replaced by the mechanism described next. MIHPS requires two parameters: a set of weight vectors W for the $R2$ indicator and the time window T_w that determines the number of times a heuristic needs to be executed. The structures C_{hh} and H_{pool} required by Algorithm 2 are initialized in line 1, and the population is randomly initialized using a uniform distribution in line 2. The main loop of MIHPS is shown in lines 3 to 17. First, two randomly-selected solutions of P create a new offspring using SBX and polynomial-based mutation in lines 4 and 5. Then, the union of P and the newly-created solution is assigned to Ψ in furtherance of ranking it using the nondominated sorting algorithm [8] in pursuance of generating a set of layers $\{L_1, \ldots, L_k\}$. L_1 has the nondominated solutions in Ψ, and L_k is composed by the worst individuals regarding the Pareto dominance relation. If the cardinality of L_k is greater than one, an IB-DE is executed. In this case, $\mathcal{Z}$, used by IGD$^+$, ϵ^+ and Δ_p, is set to L_1. Depending on the current IB-DE, the indicator contribution of each element in L_k is calculated using the proposed framework in line 10 to identify the worst contributing solution p_{min}. In line 14, the

Table 2: Properties of the WFG test problems

Problem	Separability	Frontality	Geometry
WFG1	separable	unifrontal	convex, mixed
WFG2	non-separable	$f_{1:m-1}$ unimodal f_m multimodal	convex disconected
WFG3	non-separable	unifrontal	linear, degenerated
WFG4	separable	multifrontal	concave
WFG5	separable	deceptive	concave
WFG6	non-separable	unifrontal	concave
WFG7	separable	unifrontal	concave
WFG8	non-separable	unifrontal	concave
WFG9	non-separable	multifrontal, deceptive	concave

solution p_{min} is deleted from Ψ and the resulting population is set as the population for the next iteration and assessed by the $R2$ indicator. This $R2$-value is added to the list of the current IB-DE executed. Finally, in line 21, Algorithm 2 is invoked to select, if necessary, a new IB-DE. MIHPS returns the main population as the Pareto front approximation.

Algorithm 3 MIHPS general framework

Require: Set of weight vectors W, T_w
Ensure: Pareto front Approximation
1: Initialize C_{hh} and H_{pool}
2: Randomly initialize population P
3: **while** stopping criterion is not fulfilled **do**
4: $\{p, q\} \leftarrow Select(P)$
5: offspring $\leftarrow Variation(p, q)$
6: $\Psi \leftarrow P \bigcup \{\text{offspring}\}$
7: $\{L_1, L_2, \ldots, L_k\} \leftarrow$ nondominated-sorting(Ψ)
8: **if** $|L_k| > 1$ **then**
9: $\mathcal{Z} \leftarrow L_1$
10: $\{C_i\}_{i=1,\ldots,|\mathcal{A}|} \leftarrow Contribution(L_k, W, \mathcal{Z}, C_{hh}, H_{pool})$
11: Find solution $p_{min} \in L_k$ having the minimum contribution value in $\{C_i\}_{i=1,\ldots,|\mathcal{A}|}$
12: **else**
13: p_{min} is equal to the sole individual in L_k
14: $P \leftarrow \Psi \setminus \{p_{min}\}$
15: $\delta \leftarrow -R2(P, W)$
16: $AddQualityMeasure(C_{hh}, H_{pool}, \delta)$
17: $C_{hh} \leftarrow Switch(C_{hh}, H_{pool}, T_w,)$
18: **return** P

5 EXPERIMENTAL RESULTS

In this section, we investigate the performance of MIHPS,[4] considering the nine instances of the Walking-Fish-Group (WFG) [12] test suite for 2, 3, 5, 6 and 10 objective functions. The main properties of the WFG problems are depicted in Table 2. We present two experiments: (1) a comparative study that includes the state-of-the-art algorithms MOEA/D[5] [27] (based on decomposition), NSGA-III[6] [9] (based on reference points) and $R2$-EMOA[7] [4] (based on the $R2$ indicator), and (2) an analysis of the IB-DE preference of MIHPS.

The adopted parameter values used by all MOEAs are described in Table 3. From this table, the parameter H is related to the Simplex Lattice Design (SLD) [27] that generates the set W of weight vectors required by all the MOEAs. Consequently, $|W| = C_{H-1}^{H+m-1}$. MIHPS and the selected MOEAs employ Simulated Binary Crossover (SBX) and Polynomial-based mutation (PBX) as their variation operators. For two and three objectives, the crossover probability and distribution index were set to 1.0 and 20, respectively; while for high-dimensional objective spaces, these parameters were set to 1.0 and 30. For PBX, its probability and distribution index were set to $1/n$ and 20, respectively. The stopping criterion consisted of reaching a maximum number of function evaluations of the MOP, as depicted in Table 3. The parameter T_w of MIHPS is equal to the population size, and the niche size of MOEA/D was set to 20 in all cases.

For performance assessment of the MOEAs, we selected the HV [28] and the s-energy [10] indicators. The former is focused on assessing convergence and diversity and its value is to be maximized. HV requires a reference point which for WFG1-WFG9 was set to $(2i + 1)_{i=1,2,\ldots,m}$, where m is the number of objective functions. The s-energy indicator is defined as follows:

$$E_s(\mathcal{A}) = \sum_{i \neq j} \left\| \vec{a}_i - \vec{a}_j \right\|^{-s} \tag{8}$$

where $\mathcal{A} = \{\vec{a}_1, \ldots, \vec{a}_{|\mathcal{A}|}\}$, $\vec{a}_i \in \mathbb{R}^m$, and $s > 0$ is a fixed parameter. This indicator has been used to discretize m-dimensional manifolds since its minimization leads to a uniform distribution of the points in $\mathcal{A}$, if $s \geq m$ [10].

We performed 30 independent runs of each of the four compared MOEAs using all the test instances. Tables 4, 5 and 6 show the statistical results for the HV and s-energy indicators, respectively. In these tables, the two best values among the algorithms are emphasized in grayscale, where the darker tone corresponds to the best value. A sharp symbol (#) is placed when MIHPS performed significantly better than the other approaches based on a one-tailed Wilcoxon rank sum test using a confidence level of 95%.

5.1 Comparison with state-of-the-art MOEAs

In this section, we compare MIHPS against MOEA/D, NSGA-III and $R2$-EMOA. The HV results shown in Table 4 indicate that for two objective functions, MIHPS is competitive with respect to NSGA-III which obtains the best result in 5 out of 9 problems, while MIHPS gets the best result in 4 test instances and the second best value in the remaining MOPs. In case of three objective functions, MIHPS outperforms the other algorithms, having the best value in 7 instances and the second place in the rest of MOPs. In these two objective spaces, WFG2, whose Pareto front is disconnected, presents the highest difficulty to MIHPS since it cannot obtain the best HV value. Considering MOPs having 5 and 6 objective functions, MIHPS maintains its good performance because it obtains the best value in 15 out of the 18 instances. In this regard, we observe that in both cases MIHPS obtains the best result in WFG2. Finally, when tackling 10-dimensional MOPs, MIHPS reduces its performance, although it obtains the best value in 55% of the problems. However, in WFG1, MIHPS was outperformed by MOEA/D and NSGA-III. In general, when MIHPS obtains the best value, the difference concerning NSGA-III does not look huge, although the Wilcoxon test states that the difference is indeed statistically significant. For the cases when MIHPS obtains the second place, the differences tend to be significant. Finally, the s-energy results in

[4]The source code is available at http://computacion.cs.cinvestav.mx/~jfalcon/MIHPS/mihps.html
[5]Available at http://dces.essex.ac.uk/staff/zhang/webofmoead.htm
[6]Available at http://web.ntnu.edu.tw/~tcchiang/publications/nsga3cpp/nsga3cpp.htm
[7]We employed the implementation from EMO Project 1.36 available at http://computacion.cs.cinvestav.mx/~rhernandez/

Table 3: Parameters adopted in our experiments.

Objectives (m)		2	3	5	6	10
Population size		120	120	126	126	220
Objective function evaluations ($\times 10^3$)		50	50	70	80	120
WFG	variables (n)	24	26	30	32	40
	position-related parameters	2	2	4	5	9
Weight-vector partitions (H)		119	14	5	4	3

Table 5 indicate that MIHPS has a competitive performance in low-dimensional MOPs and outperforms all the other MOEAs used in our study when dealing with many-objective problems.

5.2 Selection Bias

The probabilistic selection of an IB-DE performed by MIHPS is biased by its performance, regarding the $R2$ indicator. Consequently, it is straightforward to think that the $R2$-DE will be preferred as it intends to improve the values of $R2$ produced by the population. Our experimental results support this fact, showing that the $R2$-DE is preferred at the end of the search in almost all problem instances. However, the other IB-DEs are used at the beginning of the search. Figure 4 shows an example of the previous argument on WFG4 with three objectives. Hence, we considered necessary to determine if the combination of the indicators has an impact on the convergence of MIHPS. For this purpose, we compared MIHPS with a version of it where only $R2$-DE is turned on (denoted as MIHPS-$R2$), using the parameter values shown in Table 3. Due to space limitations, Table 6 presents the comparison regarding the HV indicator, for low-dimensional instances of the WFG test suite. It can be seen that MIHPS outperforms MIHPS-$R2$ in a statistically significant way because it obtains the best HV value in 15 out of 18 problem instances. For the three problems where MIHPS does not obtain the best result, the difference is not very significant. Hence, these results strongly support that even though $R2$-DE is mostly preferred by MIHPS, the execution of the other IB-DEs contributes to a better convergence, as confirmed by the results shown in Tables 4 and 5.

6 CONCLUSIONS AND FUTURE WORK

This paper presents a novel Multi-Indicator-based MOEA called MIHPS, which combines the strengths of four density estimators based on the use of $R2$, IGD$^+$, ϵ^+ and Δ_p. We adopted a hyper-heuristic which is on top of the algorithmic framework and is focused on learning which IB-DE is the most suitable at each moment of the search. For this purpose, a Markov chain is employed where the transition probabilities are updated based on the quality improvement or decrease of the $R2$ values in the population. $R2$ was mainly adopted because is known to be highly correlated to the hypervolume indicator but has a significantly lower computational cost. Additionally, we proposed an algorithmic framework that considerably reduces the computational cost of calculating all the contributions to the indicators and whose definition involves minimization or maximization subproblems. Experimental results indicate that the proposed approach outperforms in a statistically significant way to MOEA/D, NSGA-III and $R2$-EMOA in 31 out of 45 of the test instances adopted, regarding the HV indicator, and

Table 4: Mean and standard deviation (in parentheses) of the hypervolume indicator for the compared MOEAs and MIHPS.

Objectives	MOP	MIHPS	MOEA/D	NSGA-III	$R2$-EMOA
2	WFG1	5.353823e+00 (4.539967e-01)	5.085414e+00# (2.839145e-01)	6.627788e+00 (3.886166e-01)	4.972801e+00 # (2.120000e-01)
	WFG2	1.087631e+01 (4.043935e-01)	9.812547e+00# (5.469032e-01)	1.091544e+01 (3.990434e-01)	1.076935e+01# (3.672361e-01)
	WFG3	1.090360e+01 (1.338370e-02)	1.076476e+01# (7.102684e-02)	1.090323e+01 (1.312870e-02)	1.085161e+01# (2.379180e-02)
	WFG4	8.650363e+00 (2.063378e-02)	8.497784e+00# (2.407267e-02)	8.650159e+00# (7.209313e-03)	8.592620e+00# (2.586712e-02)
	WFG5	8.157830e+00 (3.768882e-02)	8.105310e+00# (6.867330e-03)	8.185022e+00 (3.730594e-02)	8.133849e+00# (1.887475e-02)
	WFG6	8.350939e+00 (5.352283e-02)	8.164502e+00# (1.036161e-01)	8.373642e+00 (3.334034e-02)	8.328502e+00 (3.833023e-02)
	WFG7	8.664098e+00 (2.142694e-02)	8.558870e+00# (1.836725e-02)	8.670626e+00 (3.901721e-03)	8.625866e+00# (1.282143e-02)
	WFG8	8.067041e+00 (3.917163e-02)	7.927696e+00# (3.876792e-02)	8.062539e+00 (2.129901e-02)	7.979584e+00 # (4.206135e-02)
	WFG9	8.371848e+00 (1.574505e-01)	8.097411e+00# (1.679919e-01)	8.298658e+00# (2.206774e-01)	8.238317e+00# (2.196850e-01)
3	WFG1	5.189445e+01 (1.907972e+00)	4.994533e+01# (2.615320e+00)	4.917540e+01# (1.742752e+00)	4.582011e+01# (1.903103e+00)
	WFG2	9.999710e+01 (2.691156e-01)	9.425491e+01# (1.887090e+00)	1.000303e+02 (2.020421e-01)	9.792476e+01# (4.795771e-01)
	WFG3	7.351098e+01 (8.728010e-01)	6.949014e+01# (2.043137e+00)	7.359113e+01 (3.698540e-01)	7.136640e+01# (7.927364e-01)
	WFG4	7.598303e+01 (1.185769e-01)	7.398207e+01# (3.092256e-01)	7.586556e+01# (1.753519e-01)	7.265719e+01# (3.311758e-01)
	WFG5	7.343176e+01 (3.575197e-01)	7.173103e+01# (4.978797e-01)	7.342821e+01# (1.084695e-01)	7.196333e+01# (4.816689e-01)
	WFG6	7.376195e+01 (3.751150e-01)	7.200035e+01# (6.485353e-01)	7.356399e+01# (3.730537e-01)	7.084095e+01# (6.665309e-01)
	WFG7	7.653560e+01 (7.852050e-02)	7.046696e+01# (2.114407e+00)	7.640131e+01# (8.117286e-02)	7.080832e+01# (1.568479e+00)
	WFG8	8.067041e+00 (3.917163e-02)	7.927696e+00# (3.876792e-02)	8.062539e+00 (2.129901e-02)	7.979584e+00 # (4.206135e-02)
	WFG9	7.386404e+01 (5.158326e-01)	6.675524e+01# (2.213615e+00)	7.319658e+01# (7.798323e-01)	6.578887e+01# (1.219647e+00)
5	WFG1	4.535121e+03 (1.993775e+02)	4.522924e+03 (1.145447e+02)	4.049661e+03# (1.445036e+02)	4.194966e+03# (1.358394e+02)
	WFG2	1.023085e+04 (3.828319e+01)	9.147103e+03# (2.989196e+02)	1.022660e+04 (2.444328e+01)	9.984285e+03# (6.289957e+01)
	WFG3	6.788535e+03 (6.801749e+01)	5.831355e+03# (1.740491e+02)	6.705622e+03# (6.623165e+01)	5.038991e+03# (7.488139e+02)
	WFG4	8.920978e+03 (2.213267e+01)	8.212950e+03# (2.178634e+02)	8.904989e+03# (2.089724e+01)	7.421184e+03# (2.591330e+02)
	WFG5	8.624539e+03 (1.603036e+01)	8.104988e+03# (1.012979e+02)	8.618204e+03# (1.271126e+01)	7.948213e+03# (1.147386e+02)
	WFG6	8.645060e+03 (4.070264e+01)	7.556842e+03# (1.664222e+02)	8.640890e+03 (4.979948e+01)	7.939967e+03# (8.654630e+01)
	WFG7	8.915641e+03 (4.822879e+01)	7.760876e+03# (1.586662e+02)	8.950470e+03 (1.940161e+01)	4.558253e+03# (3.763958e+02)
	WFG8	8.424204e+03 (3.017833e+01)	7.008822e+03# (3.386477e+02)	8.415246e+03 (2.900889e+01)	7.641489e+03# (7.184083e+01)
	WFG9	8.263995e+03 (1.370648e+02)	7.417024e+03# (9.145927e+02)	8.356364e+03 (1.276761e+02)	4.747704e+03# (1.345621e+03)
6	WFG1	5.480387e+04 (1.859254e+03)	5.551582e+04 (1.195407e+03)	4.624351e+04# (7.644434e+02)	4.929380e+04# (1.413982e+03)
	WFG2	1.332612e+05 (6.368992e+02)	1.178550e+05# (3.855927e+03)	1.315301e+05# (8.750023e+02)	1.300786e+05# (1.364547e+03)
	WFG3	8.454601e+04 (1.418348e+03)	6.780238e+04# (3.173871e+03)	7.863759e+04# (1.621669e+03)	4.844251e+04# (1.260649e+03)
	WFG4	1.200307e+05 (4.138230e+02)	9.790915e+04# (4.401103e+03)	1.173793e+05# (4.685098e+02)	9.324355e+04# (5.224468e+03)
	WFG5	1.162325e+05 (1.007331e+02)	1.031395e+05# (1.400494e+03)	1.148425e+05# (2.629454e+02)	1.005002e+05# (2.553915e+03)
	WFG6	1.168731e+05 (6.069773e+02)	8.312614e+04# (1.675956e+03)	1.149958e+05# (6.346863e+02)	1.046326e+05# (1.418536e+03)
	WFG7	1.207436e+05 (6.783023e+02)	8.756181e+04# (1.405257e+03)	1.188896e+05# (7.429985e+02)	5.244257e+04# (3.756718e+03)
	WFG8	1.130648e+05 (5.882422e+02)	6.120502e+04# (1.312103e+04)	1.108116e+05# (5.780063e+02)	9.887326e+04# (1.270952e+03)
	WFG9	1.109319e+05 (1.703241e+03)	8.840778e+04# (1.287881e+04)	1.095528e+05# (1.821095e+03)	3.610090e+04# (2.027429e+03)
10	WFG1	4.263671e+09 (5.387522e+07)	4.626119e+09 (9.082857e+07)	4.333786e+09 (4.767509e+07)	3.619171e+09# (4.265568e+07)
	WFG2	1.346432e+10 (4.695801e+07)	1.153362e+10# (4.307707e+08)	1.343510e+10# (5.838755e+07)	1.290151e+10# (1.470863e+08)
	WFG3	7.253349e+09 (2.738702e+08)	3.407782e+09# (4.406816e+08)	7.851751e+09 (1.420734e+08)	3.849045e+09# (7.035893e+07)
	WFG4	1.263112e+10 (1.101730e+08)	8.323219e+09# (7.081503e+08)	1.263780e+10 (8.783143e+07)	5.596499e+09# (2.750563e+08)
	WFG5	1.240345e+10 (2.216323e+07)	9.239992e+09# (2.118588e+08)	1.237722e+10# (2.716038e+07)	3.990706e+09# (1.057584e+08)
	WFG6	1.253598e+10 (6.372494e+07)	6.359273e+09# (9.586607e+08)	1.250108e+10# (5.551767e+07)	5.453261e+09# (1.016168e+09)
	WFG7	1.303975e+10 (3.716490e+07)	6.249289e+09# (5.201314e+08)	1.306886e+10 (3.687103e+07)	4.403681e+09# (1.233729e+08)
	WFG8	1.190158e+10 (7.705432e+07)	2.888315e+09# (9.700244e+08)	1.182430e+10# (9.381721e+07)	6.936492e+09# (8.189270e+08)
	WFG9	1.167146e+10 (2.269656e+08)	6.798907e+09# (2.162391e+09)	1.162166e+10# (2.416780e+08)	3.605102e+09# (1.128297e+08)

Table 5: Mean and standard deviation (in parentheses) of the s-energy indicator for the compared MOEAs and MIHPS.

Objectives	MOP	MIHPS	MOEA/D	NSGA-III	*R2*-EMOA
2	WFG1	1.872714e+07 (5.589395e+07)	2.078402e+09# (6.179776e+09)	4.220447e+08# (1.823807e+09)	3.052235e+07# (3.882580e+07)
	WFG2	1.764804e+07 (4.335797e+07)	1.360580e+11# (4.224067e+11)	7.707419e+08# (3.611565e+09)	3.652743e+07# (1.003287e+08)
	WFG3	3.500463e+05 (2.876591e+04)	4.201784e+05# (6.809222e+03)	6.939978e+06 (3.590074e+07)	4.135505e+05 (2.349694e+05)
	WFG4	7.867810e+05 (1.057606e+06)	3.489431e+05 (7.920373e+03)	5.910070e+05 (5.234480e+05)	9.951450e+05# (8.112717e+05)
	WFG5	3.567459e+05 (1.003470e+05)	4.003092e+05# (3.341154e+03)	3.741169e+05# (2.671847e+04)	1.074483e+06# (2.293603e+06)
	WFG6	8.297581e+05 (9.897593e+05)	6.037467e+07 (2.375227e+08)	8.222445e+05 (1.287128e+06)	1.185283e+07# (5.119626e+07)
	WFG7	6.005176e+05 (4.064338e+04)	3.516485e+05 (2.187221e+03)	4.151943e+05 (2.517076e+05)	2.644334e+08# (1.396116e+09)
	WFG8	9.255261e+05 (1.969640e+06)	3.489084e+05 (6.242702e+03)	6.244380e+07# (9.195854e+07)	1.143237e+06 # (7.077474e+05)
	WFG9	6.781110e+05 (4.898496e+05)	5.372987e+07 (1.257882e+08)	5.781309e+05 (5.713066e+05)	1.237779e+06 (1.588538e+06)
3	WFG1	6.143577e+07 (1.673973e+08)	8.654171e+13# (3.671307e+14)	2.001574e+11# (6.000690e+11)	1.008461e+09 (3.820614e+09)
	WFG2	6.624223e+04 (9.279462e+04)	2.397235e+12# (1.740974e+12)	5.495017e+04 (4.524221e+04)	1.443613e+08# (3.538534e+08)
	WFG3	3.520209e+08 (1.101941e+09)	3.964626e+14# (1.471524e+15)	6.718343e+13# (3.589166e+14)	3.814376e+08 (1.482391e+09)
	WFG4	1.231146e+04 (2.935879e+02)	1.901945e+04# (3.334860e+02)	1.377282e+04# (2.686847e+02)	5.462352e+04# (6.098394e+04)
	WFG5	1.117281e+04 (3.901057e+02)	1.980568e+04# (6.562792e+02)	1.325976e+04# (9.325864e+01)	8.490656e+04# (1.384068e+05)
	WFG6	7.041258e+05 (3.731772e+06)	1.886531e+04 (7.058645e+02)	8.661346e+04 (3.057806e+05)	6.563986e+06# (2.934294e+07)
	WFG7	1.139288e+04 (2.613867e+02)	1.946851e+04# (2.373307e+03)	1.332989e+04# (1.499702e+02)	6.844411e+07# (2.577339e+08)
	WFG8	6.334416e+06 (2.629782e+07)	3.223364e+04 (1.063549e+04)	5.425657e+06 (1.419605e+07)	3.641170e+06 (8.239984e+06)
	WFG9	3.184319e+04 (4.393248e+04)	6.666673e+10# (3.590110e+11)	6.667038e+10# (3.590103e+11)	3.207396e+05# (8.767693e+05)
5	WFG1	9.801655e+08 (4.316843e+09)	8.428701e+21# (3.989661e+22)	1.333338e+19# (7.180219e+19)	6.356396e+11# (3.274853e+12)
	WFG2	3.412454e+04 (1.397693e+05)	9.851610e+21# (3.854359e+22)	3.435707e+11# (1.821926e+12)	3.979127e+08# (9.931633e+08)
	WFG3	1.922689e+15 (1.034797e+16)	1.134485e+23# (6.037710e+23)	5.378389e+19# (1.542099e+20)	1.829545e+13 (8.819243e+13)
	WFG4	2.513006e+02 (1.532131e+01)	1.000468e+44# (5.385078e+44)	3.037938e+06# (8.843297e+06)	3.887261e+02 (6.295909e+02)
	WFG5	1.959483e+02 (9.455351e+00)	4.882370e+35# (9.117700e+35)	2.267384e+12# (1.138301e+13)	4.307820e+02# (1.013691e+03)
	WFG6	1.859204e+02 (1.167860e+01)	1.173885e+36 (4.338642e+36)	1.755902e+10 (8.993706e+10)	1.467884e+03 (5.302806e+03)
	WFG7	2.164027e+02 (3.118630e+01)	2.165757e+46# (7.500306e+46)	5.257040e+09# (2.069378e+10)	8.848340e+05# (2.569514e+06)
	WFG8	1.845485e+02 (1.050481e+01)	9.282909e+30# (4.513332e+31)	2.933885e+09# (1.555046e+10)	8.543378e+12 (4.600747e+13)
	WFG9	2.590924e+02 (7.018357e+01)	1.632844e+34# (7.170632e+34)	1.113532e+05# (3.526911e+05)	6.328721e+05# (1.575043e+06)
6	WFG1	6.047165e+08 (2.970199e+09)	1.146783e+25# (1.045436e+25)	6.666671e+22# (3.590110e+23)	1.078332e+12# (5.048390e+12)
	WFG2	5.221297e+03 (2.543207e+02)	7.565683e+26# (2.720479e+27)	1.905108e+12# (1.025097e+13)	5.201325e+10# (1.625235e+11)
	WFG3	1.653878e+18 (8.797877e+18)	2.000000e+23 (6.000000e+23)	1.333333e+23 (4.988877e+23)	1.204432e+03 (1.089896e+03)
	WFG4	5.609587e+01 (4.538698e+00)	7.653501e+55# (2.292190e+56)	1.354861e+14# (7.296046e+14)	3.297595e+02 (1.563612e+03)
	WFG5	3.818705e+01 (2.517843e+00)	6.406495e+43# (1.354844e+44)	2.530719e+09# (8.470160e+09)	1.927523e+02 (5.843129e+02)
	WFG6	3.465443e+01 (2.886772e+00)	9.787867e+43# (3.027649e+44)	6.666667e+22# (3.590110e+23)	8.009979e+02 (3.432225e+03)
	WFG7	4.038720e+01 (4.437763e+00)	6.635666e+55# (2.699486e+56)	1.087107e+12# (5.838292e+12)	7.460269e+04# (3.384252e+05)
	WFG8	3.997036e+01 (4.850055e+00)	3.528092e+36# (1.620639e+37)	6.666667e+22# (3.590110e+23)	1.833067e+02 (7.276364e+02)
	WFG9	4.452187e+01 (1.485791e+01)	4.653538e+42# (2.441525e+43)	4.219370e+05# (1.138974e+06)	9.827496e+06# (5.228468e+07)
10	WFG1	6.025963e+07 (4.819117e+07)	1.334400e+59# (7.180024e+59)	2.666667e+39# (1.123487e+40)	3.801374e+13# (1.496857e+14)
	WFG2	1.805484e+04 (4.251975e+03)	1.600000e+60# (8.616264e+60)	6.939858e+30# (3.712175e+31)	3.715520e+20# (2.000830e+21)
	WFG3	1.352050e+04 (7.158030e+04)	3.968305e+49# (1.575951e+50)	4.695580e+39# (1.121605e+40)	1.014720e+01 (1.772339e+00)
	WFG4	3.429733e+00 (2.657303e+00)	7.893333e+111# (4.250690e+112)	4.071902e+00# (1.264681e+00)	2.097761e+01# (2.430840e+01)
	WFG5	1.266066e+00 (1.792841e-01)	2.438414e+72# (5.575768e+72)	3.892117e+00# (2.723236e-01)	2.960655e+02# (3.920714e+02)
	WFG6	1.082768e+00 (1.733274e-01)	6.860262e+71# (3.694218e+72)	3.985430e+00# (3.971706e-01)	1.323056e+06# (6.788670e+06)
	WFG7	1.381504e+00 (2.415390e-01)	2.572763e+102# (9.786282e+102)	3.869951e+00# (4.029032e-01)	3.825779e+01# (6.971002e+01)
	WFG8	3.184230e+00 (2.265388e+00)	2.055197e+62# (6.219703e+62)	3.212638e+01# (1.459811e+02)	9.061778e+03# (4.659196e+04)
	WFG9	2.201585e+00 (2.067237e+00)	4.338407e+70# (1.149034e+71)	8.802783e+00# (8.806394e+00)	2.885282e+01# (3.981606e+01)

Figure 3: Pareto fronts produced by MIHPS. All fronts correspond to the HV median.

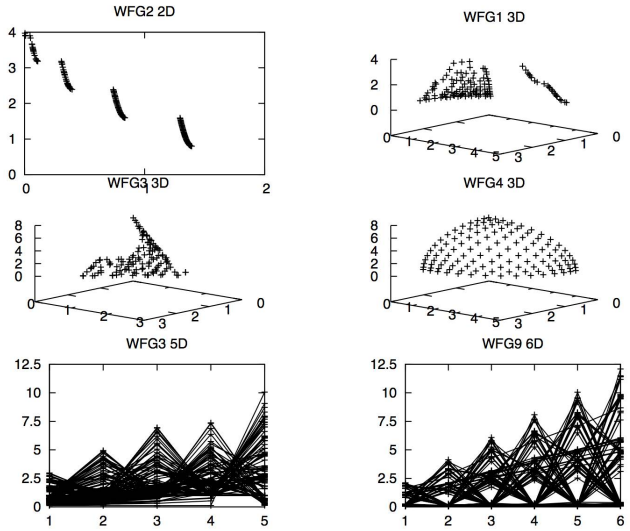

Table 6: Mean and standard deviation (in parentheses) of the hypervolume indicator for MIHPS and MIHPS-*R2*.

Objectives	MOP	MIHPS	MIHPS-*R2*
2	WFG1	5.353823e+00 (4.539967e-01)	4.909215e+00# (2.354320e-01)
	WFG2	1.087631e+01 (4.043935e-01)	1.088208e+01 (4.060801e-01)
	WFG3	1.090360e+01 (1.338370e-02)	1.083356e+01# (3.044440e-02)
	WFG4	8.650363e+00 (2.063378e-02)	8.584441e+00# (2.619502e-02)
	WFG5	8.157830e+00 (3.768882e-02)	8.132564e+00# (1.937931e-02)
	WFG6	8.350939e+00 (5.352283e-02)	8.305956e+00# (4.739550e-02)
	WFG7	8.664098e+00 (2.142694e-02)	8.620447e+00# (2.985012e-02)
	WFG8	8.067041e+00 (3.917163e-02)	7.986139e+00# (3.097071e-02)
	WFG9	8.371848e+00 (1.574505e-01)	8.263080e+00# (1.838899e-01)
3	WFG1	5.189445e+01 (1.907972e+00)	5.188408e+01 (1.610899e+00)
	WFG2	1.085075e+01 (3.864759e-01)	1.088208e+01 (4.060801e-01)
	WFG3	7.351098e+01 (8.728010e-01)	7.302124e+01# (3.418580e-01)
	WFG4	7.598303e+01 (1.185769e-01)	7.594650e+01# (1.511291e-01)
	WFG5	7.343176e+01 (3.575197e-01)	7.347454e+01 (9.055205e-02)
	WFG6	7.376195e+01 (3.751150e-01)	7.358466e+01# (3.801285e-01)
	WFG7	7.653560e+01 (7.852050e-02)	7.648279e+01# (7.837593e-02)
	WFG8	7.265162e+01 (2.082143e-01)	7.261357e+01# (1.609685e-01)
	WFG9	7.386404e+01 (5.158326e-01)	7.346278e+01# (9.396951e-01)

in 34 out of 45 MOPs considering the s-energy indicator. Based on these results, we believe that MIHPS is a suitable alternative for solving multi-objective optimization problems having both few or many objectives. As part of our future work, we are interested in studying the particular effect of each IB-DE to understand their specific contributions to the search process and to characterize their convergence and distribution features empirically. Finally, we would like to investigate the effect of the values adopted to update the transition probabilities of the Markov chain.

Figure 4: IB-DE preference on WFG4 with 3 objective functions. Since MIHPS is a steady-state MOEA, the number of generations is equivalent to the number of function evaluations.

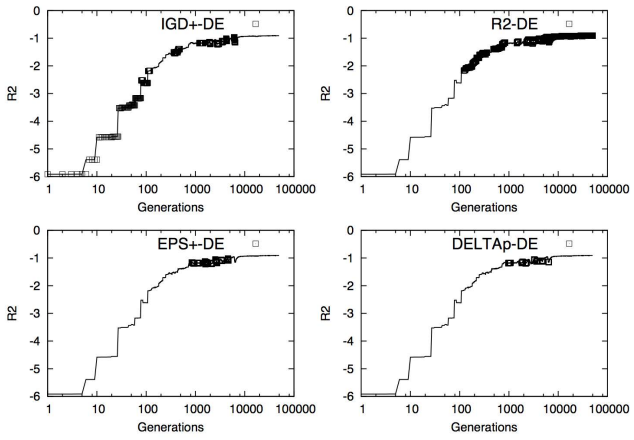

ACKNOWLEDGMENTS

The first author acknowledges support from CINVESTAV-IPN and CONACyT to pursue graduate studies in Computer Science. The second author gratefully acknowledges support from CONACyT project no. 221551.

REFERENCES

[1] Johannes Bader and Eckart Zitzler. 2011. HypE: An Algorithm for Fast Hypervolume-Based Many-Objective Optimization. *Evolutionary Computation* 19, 1 (Spring 2011), 45–76.

[2] Nicola Beume, Boris Naujoks, and Michael Emmerich. 2007. SMS-EMOA: Multiobjective selection based on dominated hypervolume. *European Journal of Operational Research* 181, 3 (16 September 2007), 1653–1669.

[3] Dimo Brockhoff, Tobias Wagner, and Heike Trautmann. 2012. On the Properties of the *R2* Indicator. In *2012 Genetic and Evolutionary Computation Conference (GECCO'2012)*. ACM Press, Philadelphia, USA, 465–472. ISBN: 978-1-4503-1177-9.

[4] Dimo Brockhoff, Tobias Wagner, and Heike Trautmann. 2015. R2 Indicator-Based Multiobjective Search. *Evolutionary Computation* 23, 3 (Fall 2015), 369–395.

[5] Edmund K Burke, Michel Gendreau, Matthew Hyde, Graham Kendall, Gabriela Ochoa, Ender Özcan, and Rong Qu. 2013. Hyper-heuristics: a survey of the state of the art. *Journal of the Operational Research Society* 64, 12 (01 Dec 2013), 1695–1724.

[6] Carlos A. Coello Coello and Nareli Cruz Cortés. 2002. An Approach to Solve Multiobjective Optimization Problems Based on an Artificial Immune System. In *First International Conference on Artificial Immune Systems (ICARIS'2002)*, Jonathan Timmis and Peter J. Bentley (Eds.). University of Kent at Canterbury, UK, 212–221. ISBN 1-902671-32-5.

[7] Carlos A. Coello Coello, Gary B. Lamont, and David A. Van Veldhuizen. 2007. *Evolutionary Algorithms for Solving Multi-Objective Problems* (second ed.). Springer, New York. ISBN 978-0-387-33254-3.

[8] Kalyanmoy Deb, Samir Agrawal, Amrit Pratap, and T. Meyarivan. 2000. A Fast Elitist Non-Dominated Sorting Genetic Algorithm for Multi-Objective Optimization: NSGA-II. In *Proceedings of the Parallel Problem Solving from Nature VI Conference*, Marc Schoenauer, Kalyanmoy Deb, Günter Rudolph, Xin Yao, Evelyne Lutton, Juan Julian Merelo, and Hans-Paul Schwefel (Eds.). Springer. Lecture Notes in Computer Science No. 1917, Paris, France, 849–858.

[9] Kalyanmoy Deb and Himanshu Jain. 2014. An Evolutionary Many-Objective Optimization Algorithm Using Reference-Point-Based Nondominated Sorting Approach, Part I: Solving Problems With Box Constraints. *IEEE Transactions on Evolutionary Computation* 18, 4 (August 2014), 577–601.

[10] D. P. Hardin and E. B. Saff. [n. d.]. Discretizing Manifolds via Minimum Energy Points. *Notices of the AMS* 51, 10 ([n. d.]), 1186–1194.

[11] Raquel Hernández Gómez and Carlos A. Coello Coello. 2017. A Hyper-Heuristic of Scalarizing Functions. In *2017 Genetic and Evolutionary Computation Conference (GECCO'2017)*. ACM Press, Berlin, Germany, 577 –584. ISBN 978-1-4503-4920-8.

[12] Simon Huband, Luigi Barone, Lyndon While, and Phil Hingston. 2005. A Scalable Multi-objective Test Problem Toolkit. In *Evolutionary Multi-Criterion Optimization. Third International Conference, EMO 2005*, Carlos A. Coello Coello, Arturo Hernández Aguirre, and Eckart Zitzler (Eds.). Springer. Lecture Notes in Computer Science Vol. 3410, Guanajuato, México, 280–295.

[13] Hisao Ishibuchi, Hiroyuki Masuda, Yuki Tanigaki, and Yusuke Nojima. 2015. Modified Distance Calculation in Generational Distance and Inverted Generational Distance. In *Evolutionary Multi-Criterion Optimization, 8th International Conference, EMO 2015*, António Gaspar-Cunha, Carlos Henggeler Antunes, and Carlos Coello Coello (Eds.). Springer. Lecture Notes in Computer Science Vol. 9019, Guimarães, Portugal, 110–125.

[14] Hisao Ishibuchi, Noritaka Tsukamoto, and Yusuke Nojima. 2008. Evolutionary many-objective optimization: A short review. In *2008 Congress on Evolutionary Computation (CEC'2008)*. IEEE Service Center, Hong Kong, 2424–2431.

[15] Siwei Jiang, Yew-Soon Ong, Jie Zhang, and Liang Feng. 2014. Consistencies and Contradictions of Performance Metrics in Multiobjective Optimization. *IEEE Transactions on Cybernetics* 44, 12 (December 2014), 2391–2404.

[16] Joshua Knowles and David Corne. 2002. On Metrics for Comparing Nondominated Sets. In *Congress on Evolutionary Computation (CEC'2002)*, Vol. 1. IEEE Service Center, Piscataway, New Jersey, 711–716.

[17] Joshua Knowles and David Corne. 2003. Properties of an Adaptive Archiving Algorithm for Storing Nondominated Vectors. *IEEE Transactions on Evolutionary Computation* 7, 2 (April 2003), 100–116.

[18] Bingdong Li, Ke Tang, Jinlong Li, and Xin Yao. 2016. Stochastic Ranking Algorithm for Many-Objective Optimization Based on Multiple Indicators. *IEEE Transactions on Evolutionary Computation* 20, 6 (December 2016), 924–938.

[19] Miqing Li, Shengxiang Yang, and Xiaohui Liu. 2014. Shift-Based Density Estimation for Pareto-Based Algorithms in Many-Objective Optimization. *IEEE Transactions on Evolutionary Computation* 18, 3 (June 2014), 348–365.

[20] Arnaud Liefooghe and Bilel Derbel. 2016. A Correlation Analysis of Set Quality Indicator Values in Multiobjective Optimization. In *2016 Genetic and Evolutionary Computation Conference (GECCO'2016)*. ACM Press, Denver, Colorado, USA, 581–588. ISBN 978-1-4503-4206-3.

[21] Kent McClymont and Ed C. Keedwell. 2011. Markov Chain hyper-Heuristic (MCHH): an Online Selective Hyper-Heuristic for Multi-Objective Continuous Problems. In *2011 Genetic and Evolutionary Computation Conference (GECCO'2011)*. ACM Press, Dublin, Ireland, 2003–2010.

[22] Tatsuya Okabe, Yaochu Jin, and Bernhard Sendhoff. 2003. A Critical Survey of Performance Indices for Multi-Objective Optimization. In *Proceedings of the 2003 Congress on Evolutionary Computation (CEC'2003)*, Vol. 2. IEEE Press, Canberra, Australia, 878–885.

[23] Dung H. Phan and Junichi Suzuki. 2011. Boosting Indicator-based Selection Operators for Evolutionary Multiobjective Optimization Algorithms. In *2011 23rd IEEE International Conference on Tools with Artificial Intelligence*. IEEE press, 276–281.

[24] Dung H. Phan, Junichi Suzuki, and Isao Hayashi. 2012. Leveraging Indicator-Based Ensemble Selection in Evolutionary Multiobjective Optimization Algorithms. In *2012 Genetic and Evolutionary Computation Conference (GECCO'2012)*. ACM Press, Philadelphia, USA, 497–504. ISBN: 978-1-4503-1177-9.

[25] Oliver Schütze, Xavier Esquivel, Adriana Lara, and Carlos A. Coello Coello. 2012. Using the Averaged Hausdorff Distance as a Performance Measure in Evolutionary Multiobjective Optimization. *IEEE Transactions on Evolutionary Computation* 16, 4 (August 2012), 504–522.

[26] David A. Van Veldhuizen. 1999. *Multiobjective Evolutionary Algorithms: Classifications, Analyses, and New Innovations.* Ph.D. Dissertation. Department of Electrical and Computer Engineering. Graduate School of Engineering. Air Force Institute of Technology, Wright-Patterson AFB, Ohio, USA.

[27] Qingfu Zhang and Hui Li. 2007. MOEA/D: A Multiobjective Evolutionary Algorithm Based on Decomposition. *IEEE Transactions on Evolutionary Computation* 11, 6 (December 2007), 712–731.

[28] Eckart Zitzler. 1999. *Evolutionary Algorithms for Multiobjective Optimization: Methods and Applications.* Ph.D. Dissertation. Swiss Federal Institute of Technology (ETH), Zurich, Switzerland.

[29] Eckart Zitzler, Kalyanmoy Deb, and Lothar Thiele. 2000. Comparison of Multiobjective Evolutionary Algorithms: Empirical Results. *Evolutionary Computation* 8, 2 (Summer 2000), 173–195.

[30] Eckart Zitzler and Simon Künzli. 2004. Indicator-based Selection in Multiobjective Search. In *Parallel Problem Solving from Nature - PPSN VIII*, Xin Yao et al. (Ed.). Springer-Verlag. Lecture Notes in Computer Science Vol. 3242, Birmingham, UK, 832–842.

[31] Eckart Zitzler and Lothar Thiele. 1998. Multiobjective Optimization Using Evolutionary Algorithms—A Comparative Study. In *Parallel Problem Solving from Nature V*, A. E. Eiben (Ed.). Springer-Verlag, Amsterdam, 292–301.

[32] Eckart Zitzler, Lothar Thiele, Marco Laumanns, Carlos M. Fonseca, and Viviane Grunert da Fonseca. 2003. Performance Assessment of Multiobjective Optimizers: An Analysis and Review. *IEEE Transactions on Evolutionary Computation* 7, 2 (April 2003), 117–132.